Sound Absorption Measurements for Micro-Perforated Plates: The Effect of Edge Profile

Muttalip Aşkın Temiz
Department of Mechanical Engineering, Eindhoven University of Technology, Eindhoven, the Netherlands.

Ines Lopez Arteaga
Department of Mechanical Engineering, Eindhoven University of Technology, Eindhoven, the Netherlands.

Avraham Hirschberg
Department of Applied Physics, Eindhoven University of Technology, Eindhoven, the Netherlands.

Summary
In this study, the effect of perforation edge profile in micro-perforated plates (MPPs) is investigated and compared with the sharp edge case. MPPs are metal plates with small holes (perforations) that absorb incident sound waves using the Stokes boundary layers developed inside and in the vicinity of the perforations. The perforation diameter should be optimized so that the Stokes layers cover almost the entire perforation thus maximizing the absorbed sound energy due to viscosity. Hence, designing MPPs is a tuning problem. The existing analytical model for evaluating the transfer impedance of the MPPs is based on the assumption that the edge profiles of the perforations are sharp. In other words, the angle between the plate surface and the inner surface of the perforation is 90°;. This case is not very practical to achieve in mass production of MPPs, since the perforations are formed by drilling and / or punching in manufacturing. To investigate the effect of the edge profile on the performance of the MPP, we design samples with different edge profiles such as sharp and 45°-chamfers on both edges. We carry out open-end reflection coefficient measurements in a semi-anechoic room with 6 microphones. The relative error of this setup is measured to be less than 0.5% for closed-end reflection coefficient between 100 Hz and 700 Hz in the linear regime. The measurements are also compared with a linear numerical model. In our measurements, we observe that the edge profile can have an effect up to 30% in resistance and 18% in reactance.

PACS no. 43.20.El, 43.58.Bh

1. Introduction

Micro-perforated plates are metal plates with low porosity, $\sigma = \mathcal{O}(1\%)$, and small perforation diameter, $d_p = \mathcal{O}(1\,mm)$. Due to the small diameter size of the perforations, flow oscillations form a Stokes boundary layer whose thickness, δ_v, is comparable with the radius of the perforation. When backed by a cavity, this resistance effectively absorbs incident acoustic waves in a frequency range determined by the volume of the cavity. The parameters defining an MPP are shown in Figure 1.

The absorption properties of the MPPs were first investigated by Maa[5]. He assumed the neighbouring perforations do not affect each other due to low porosity and bases his study on the impedance of a single perforation. Maa combines Kirchhoff's[1] analytical model for the oscillating viscous flow in an infinitely long capillary tube with Ingard's[2] expressions for end-corrections in infinitely thin orifices. Since Ingard bases his calculations on thin Stokes layer assumption, there is a discrepancy between Maa's model and experiment results. This discrepancy has been linked to the perforation edge geometry[8] and different end-correction coefficients for sharp and rounded profiles are suggested. A recent study[9] shows that even for the same geometry, *i.e.* sharp edge profile, the end-correction coefficients vary as a function of the Shear number, Sh, which is the ratio of the perforation radius to the Stokes layer thickness.

(c) European Acoustics Association

Copyright© (2015) by EAA-NAG-ABAV, ISSN 2226-5147
All rights reserved

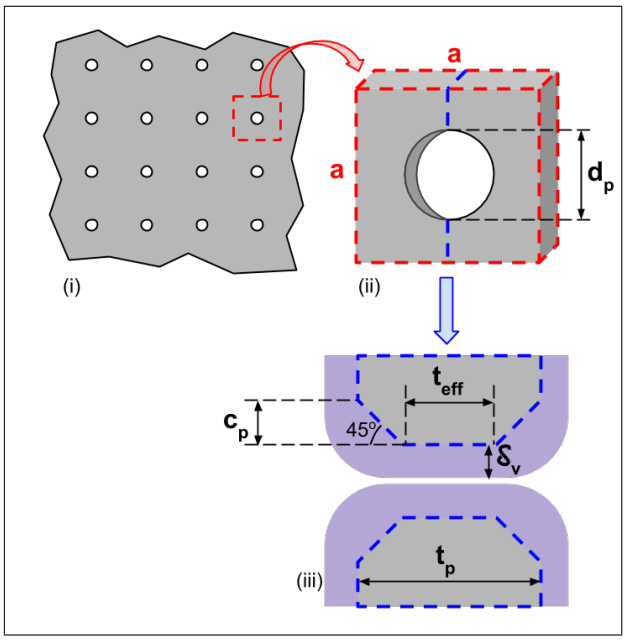

Figure 1. (i) A fragment of an MPP, (ii) zooming on a single perforation and (iii) cross-section of a single perforation with both-ends-chamfered profile. The parameters are shown in the figure as well: perforation diameter d_p, plate thickness t_p, effective plate thickness t_{eff}, chamfer length c_p, Stokes layer thickness δ_v and lattice parameter a. Porosity of the plate is $\sigma = d_p^2\pi/(4a^2)$.

This study aims at investigating the effect of the edge profile on the acoustic properties of a single perforation by means of open end impedance measurements. Instead of rounded edge profile, we use chamfered edges for their size is easier to control in the manufacturing process. We compare the transfer impedance of the samples with different chamfer sizes with the sharp edge case in the linear regime.

2. Theory

In this study, the transfer impedance of an MPP is deduced from reflection coefficient measurements. Under planar wave assumption, the reflection coefficient, R, and the impedance, Z, of a duct termination can be related as follows:

$$Z(f) = \rho_0 c_0 \frac{1+R(f)}{1-R(f)}, \tag{1}$$

where ρ_0 and c_0 are the density and speed of sound of air in this study; f is the frequency. The impedance Z and the reflection coefficient R are both complex quantities. R is not directly measured in the impedance tube. It is calculated from the complex pressure amplitudes using the multi-microphone method[6].

Assuming the tube termination as the reference, $x = 0$, the complex pressure amplitude at position x is decomposed into right and left traveling waves.

$$\hat{p}(f,x) = \hat{p}_+(f)e^{(-jk_+x)} + \hat{p}_-(f)e^{(jk_-x)}, \tag{2}$$

where, $\hat{p}$ is the complex pressure amplitude, j is the imaginary number $\sqrt{-1}$, k is the complex wave number and subscripts '+' and '−' indicate the right and left traveling waves respectively. In the absence of steady flow, $k = k_+ = k_-$. Considering the viscothermal effects in the tube, k is approximated by Peters et al.[4] as:

$$\begin{aligned} k = &\frac{\omega}{c_0}\left[1 + \frac{1-j}{\sqrt{2}}\frac{1}{Sh_D}\left(1+\frac{\gamma-1}{Pr^{0.5}}\right)\right] \\ &- \frac{\omega}{c_0}\frac{j}{Sh_D^2}\left(1+\frac{\gamma-1}{Pr^{0.5}} - \frac{1}{2}\gamma\frac{\gamma-1}{Pr}\right). \end{aligned} \tag{3}$$

In Eq. 3, $\omega = 2\pi f$ is the angular frequency, γ and Pr are respectively ratio of the specific heats and Prandtl number. $Sh_D = D\sqrt{\omega\rho_0/4\mu}$ is the Shear number where D is the diameter of the impedance tube, ρ_0 is the density of air and μ is the dynamic viscosity of air.

Once the wave decomposition is obtained, $R(f)$ at the tube termination ($x = 0$) is computed.

$$R(f) = \hat{p}_-(f)/\hat{p}_+(f). \tag{4}$$

From Eq. 2, one can see that a measurement with 2 microphones could be enough to determine the complex pressure amplitudes, $\hat{p}_+$ and $\hat{p}_-$, at $x = 0$. Yet, increasing the number of microphones results in an over-determined set of equations whose solution is less sensitive to errors than the 2-microphone method [6]. For instance, for a measurement containing n frequency steps, our 6-microphone impedance tube setup produces a set of $6n$ equations which needs to be solved for $2n$ unknowns, *i.e.* $\hat{p}_+$ and $\hat{p}_-$ for each frequency step. The supplementary information coming from the extra microphones serves for other purposes such as measuring the speed of sound, c_0. Aurégan and Leroux[7] introduces c_0 as an additional unknown to this set of $6n$ equations to solve $2n+1$ unknowns. Considering that c_0 is sensitive to humidity and temperature, measuring it directly reduces the measurement errors.

3. Experimental Method

The impedance tube and the complementary items of the experiment are sketched in Figure 2.

The tube shown in Figure 2 is 1-m long and the inner diameter is $D = 50mm$. Along the tube, there are 6 *BSWA MPA416* mirophones that are placed

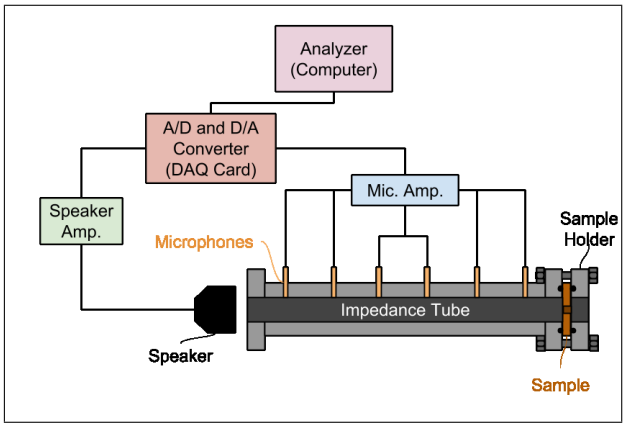

Figure 2. The schematic drawing of the experiment setup.

equidistantly. The distance between two neighbouring microphones is 175 mm and their sensitivity is about 51 mV/Pa.

We perform signal processing and data acquision with the combination of *NI PCIe-6361 X-Series* DAQ card and LabView. The sampling frequency for generated excitation signal is 20 kHz where the recording sampling frequency is 10 kHz. For each frequency step, we record the data for 10 seconds and trim the first and last 2 seconds to exclude transient effects. The recorded pressure data is transformed into the Frequency domain with a Lock-in method. A separate Matlab script has been built for this post-processing.

Since we perform reflection coefficient measurements, relative calibration of the microphones is sufficeint. In the calibration process, all the microphones are placed at the same distance with respect to the speaker and for each frequency step in the region $100\,\text{Hz} < f < 700\,\text{Hz}$, a calibration coefficient is measured relative to a reference microphone.

To avoid a temperature gradient inside the tube, after each 20 frequency-steps, we wait 15 minutes for the temperature to uniformize again.

With all of the precautions and methods employed, in the frequency range of $100\,\text{Hz} < f < 700\,\text{Hz}$, the error is less than 0.5% for closed-end reflection coefficient measurements. Yet, we perform open-end measurements to calculate the transfer impedance of an MPP sample. The idea behind the *open-end transfer impedance measurement* is illustrated in Figure 3.

We perform open-end measurements in a semi-anechoic room to minimize the effect of ambiance. Since both the *open-end* and *sample loaded open-end* measurements are carried out in the same medium, we expect the radiation impedance to be the same for both of the cases. Moreover, recalling that the porosity of the samples are in the order of 1%, the transfer impedance of the samples are expected to be much larger than the radiation impedance.

We use 3 samples whose perforation diameter, d_p, plate thikness, t_p, and porosity, σ, values are identical. The only difference between these samples is the chamfer length, c_p. (See Table I.)

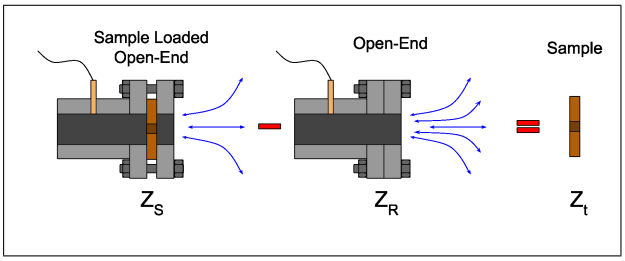

Figure 3. Open-end transfer impedance measurements. The difference between sample loaded termination impedance, Z_S, and open termination impedance, Z_R, gives the transfer impedance of the plate, $Z_t = Z_S - Z_R$.

Table I. Specifications of the geometry of the samples.

Sample	$d_p[mm]$	$t_p[mm]$	σ [%]	$c_p[mm]$
A	4.2 ± 0.01	4.0 ± 0.01	0.71	0
B	4.2 ± 0.01	4.0 ± 0.01	0.71	0.35 ± 0.01
C	4.2 ± 0.01	4.0 ± 0.01	0.71	1.00 ± 0.01

In MPPs, the ratio of the perforation to the fluid particle displacement defines if the response is linear or non-linear. This ratio is known as *Strouhal number* and calculated as $Sr = \omega d_p/|\hat{u}_p|$ [3] where the velocity is calculated as $\hat{u}_p = (\hat{p}_+ - \hat{p}_-)/(\rho_0 c_0 \sigma)$. Since Sr increases with increasing frequency, we check the linearity of our experiments prior to each measurement. This is done by decreasing the amplitude of the excitation gradually at the lowest frequency, *i.e.* 100 Hz. When two successive measurements have the same reflection coefficient, we continue the measurement with increasing frequencies.

4. Results and Discussions

We checked the accuracy of our impedance tube with a closed-end reflection coefficient measurement. The amplitude and the phase of R are shown in Figures 4 and 5.

For the amplitude $|R|$, the measured data points are randomly distributed above and below the theoretical value, *i.e.* $|R| = 1.000$. Yet, around $600\,Hz$ there is a significant deviation in the accuracy of the measurement. In general, the error of the randomly distributed points are within a 0.5% band. This sharp change in the reflection coefficient around $600\,Hz$ may be due to a mechanical resonance of the impedance tube setup. The measurement points for phase of R are randomly distributed around 0 with deviations of about $2 \times 10^{-3}\,rad$, corresponding to an uncertainity of $1\,mm$ at $100\,Hz$.

Based on this accuracy, we carry out the *open-end transfer impedance measurements* with the samples. The normalized resistance and reactance values of the three samples are plotted in Figures 6 and 7.

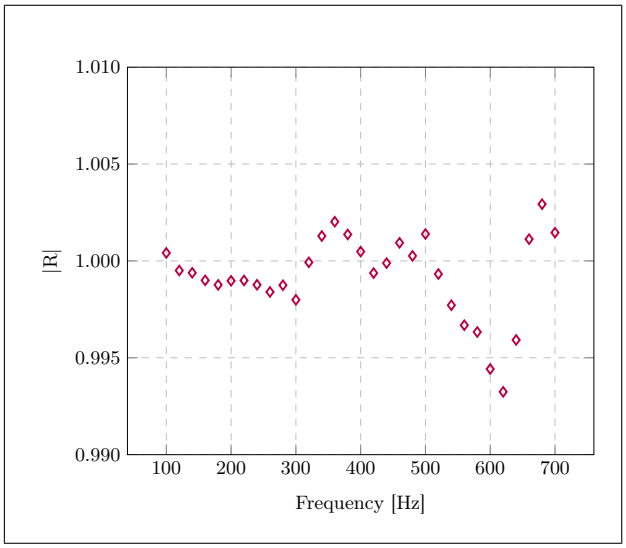

Figure 4. The amplitude of the reflection coefficient measured for the impedance tube with a closed-end termination. Except from two data points around $600Hz$, all the measured values are within the 0.5% error band.

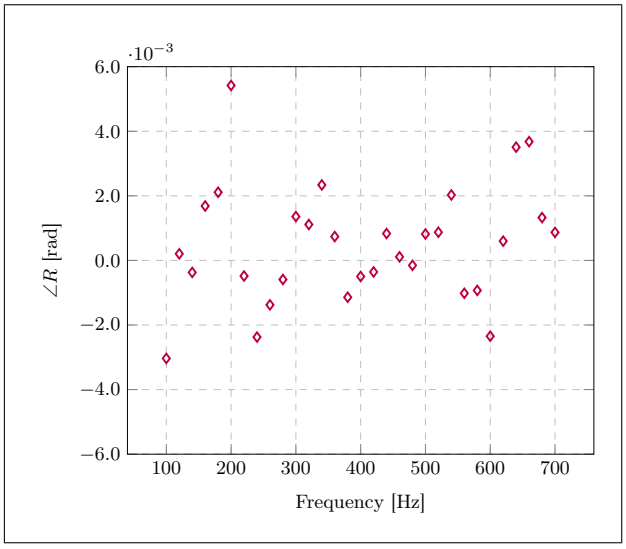

Figure 5. The phase of the reflection coefficient measured for the impedance tube with a closed-end termination. The measured points are randomly distributed around 0, with a scatter of $2 \times 10^{-3}\, rad$.

We solve the linearized incompressible Navier-Stokes equations numerically for Sample A. The description of these calculations is provided by Temiz et al. [9]. The simulations and the experiments are comparable up to $Sh \approx 30$ with $Sh = d_p\sqrt{\omega\rho_0/(4\mu)}$. Although this verifies the measurement method, the scattering behaviour of the experiment results for $Sh > 30$ should be investigated further.

With chamfers, the length of the narrowest section of the MPP, t_{eff}, reduces. This narrow section is the part where the resistance is maximum and defined as *effective plate thickness*, $t_{eff} = t_p - 2c_p$. The gradual area change at the chamfered section of the perforation still contributes to the resistance, but it is not as much as the contribution from neck section. The result of this change is observed in Figure 6. In our measurements, the resistance of Sample C is 30 % less than that of Sample A.

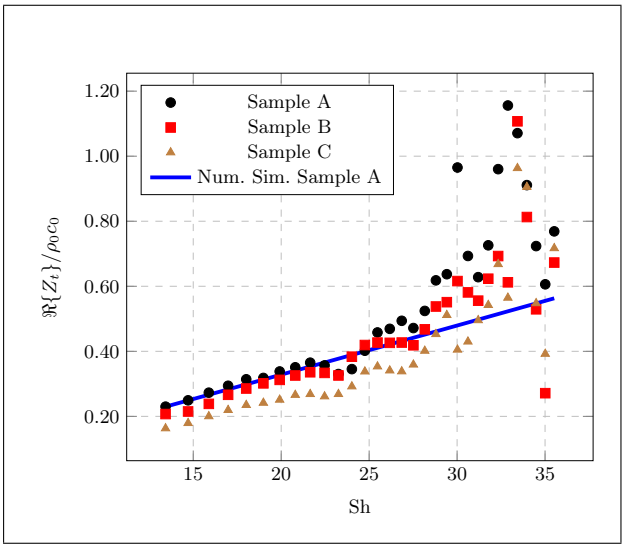

Figure 6. The change in resistance of a perforation for different chamfer lengths. The measured resistance is normalized with respect to $\rho_0 c_0$.

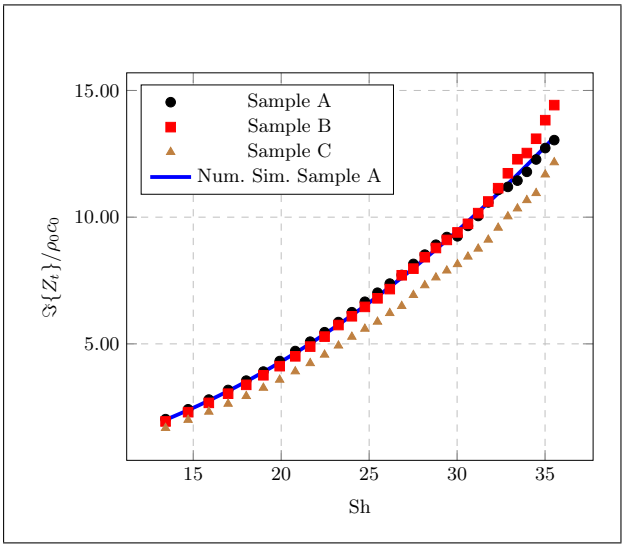

Figure 7. The change in reactance of a perforation for different chamfer lengths. The measured reactance is normalized with respect to $\rho_0 c_0$.

The reactance of the perforation is reduced with increasing chamfer size as well. The gradual change of the area causes a reduction in the oscillating *effective mass*. The effect of the chamfering is not as strong as in the resistance in our experiments, but it still causes a up to 18 % for a chamfer length of $c_p = d_p/4.2$.

In Figures 6 and 7, we notice scattering of the data for $Sh \geq 30$. For the samples used, this corresponds to $f \geq 600\, Hz$. Some precautions have been taken to evade this effect, such as carrying out the measure-

ments in the semi-anechoic chamber, trying different loudspeakers, using various lengths of sample holders, increasing the stiffness of the supporting frame of the impedance tube, etc. Yet, this scattering is still observed in the measurements. This is an aspect of the study which should be improved.

5. Conclusions

We have carried out open-end reflection coefficient measurements in the linear regime to determine the transfer impedance of a single perforation. The focus of this study is the effect of edge profiles with 45°-chamfers. We have measured the change in transfer impedance in samples with different chamfer sizes.

The most noticeable observation of this study is that the chamfered edge profile leads to a significant decrease in both resistance and reactance of a perforation. For instance, compared to the sharp-edge profile, both-ends-chamfered profile with a chamfer length of $c_p = d_p/4.2$ reduces the resistance and the reactance up to 30 % and 18 % respectively.

Even though this study has been carried out using samples with chamfered-edge profiles, the change in the transfer impedance indicates the importance of the edge profile effect on MPPs. Therefore, these effects should be modeled accurately in calculations.

Acknowledgement

The presented work is part of the Marie Curie Initial Training Network Thermo-acoustic and aero-acoustic nonlinearities in green combustors with orifice structures (TANGO). We gratefully acknowledge the financial support from the European Commission under call FP7-PEOPLE-ITN-2012.

References

[1] G. Kirchhoff: Uber der einfluss der wärmeleitung in einem gase auf die schallbewagung, Annalen der Physik and Chemie 134 (1868) 177-193.

[2] U. Ingard: On the Theory and Design of Acoustic Resonators, J. Acoust. Soc. Am. 25 (1953) 1037-1061.

[3] U. Ingard, H. Ising: Acoustic Non-Linearity of an Orifice, J. Acoust. Soc. Am. 42 (1967) 6-17.

[4] M.C.A.M. Peters, A. Hirschberg, A.J. Reijnen, A.P.J. Wijnands: Damping and reflection coefficient measurements for an open pipe at low Mach and low Helmholtz numbers, J. Fluid Mech. 256 (1993) 499-534.

[5] D.-Y. Maa: Potential of Microperforated Panel Absorber, J. Acoust. Soc. Am. 104 (1998) 2861-2866.

[6] S.-H. Jang, J.-G. Ih: On the multiple microphone method for measuring in-duct acoutic properties in the presence of mean flow, J. Acoust. Soc. Am. 103 (1998) 1520-1526.

[7] Y. Aurégan, M. Leroux: Failures in the discrete models for flow duct with perforations: an experimental investigation, Journal of Sound and Vibrations 265 (2003) 109-121.

[8] S. Allam, M. Åbom: A New Type of Muffler Based on Microperforated Tubes, Journal of Vibration and Acoustics 113 (2011) 1-8.

[9] M.A. Temiz, I. Lopez Arteaga, G. Efraimsson, M. Åbom, A. Hirschberg: Acoustic End Correction in Micro-Perforated Plates - Revisited. Proc. ICSV-21 2014, 1-7.